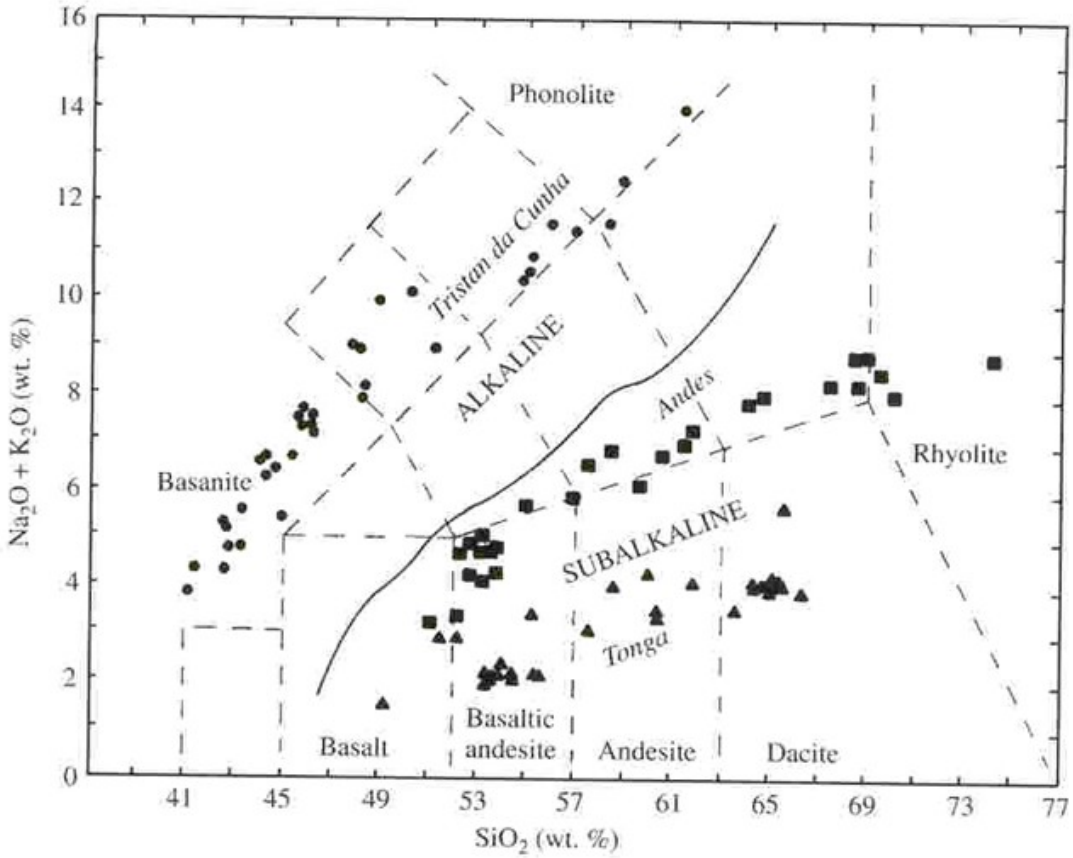

2.16 Total alkalies-silica diagram showing fields and examples of **subalkaline** and **alkaline rock suites.** Irregular solid line separates the field of nepheline-normative rocks from rocks having no normative nepheline in the 15,164-sample database of Le Bas et al., (1992). Light dashed lines delineate the IUGS volcanic rock-type classification from Figure 2.12. Note that a single rock type, such as basalt, can be either alkaline (*Ne*-normative) or subalkaline (*Hy*-normative). The alkaline volcanic suite of basanite, phonotephrite, tephriphonolite, and phonolite (filled circles) is from Tristan da Cunha, a volcanic oceanic island near the intersection of the Mid-Atlantic and Walvis Ridges in the South Atlantic Ocean (Le Roex et al., 1990). The subalkaline volcanic suite from the oceanic island arc of Tonga (filled triangles) is mostly basaltic andesite, andesite, and dacite (Cole, 1982). Subalkaline-suite rocks from Volcan Descabezado Grande and Cerro Azul in the southern volcanic zone of the Andes in central Chile (filled squares) are mostly basaltic andesite, trachyandesite, trachydacite, and rhyolite (Hildreth and Moorbath, 1988).

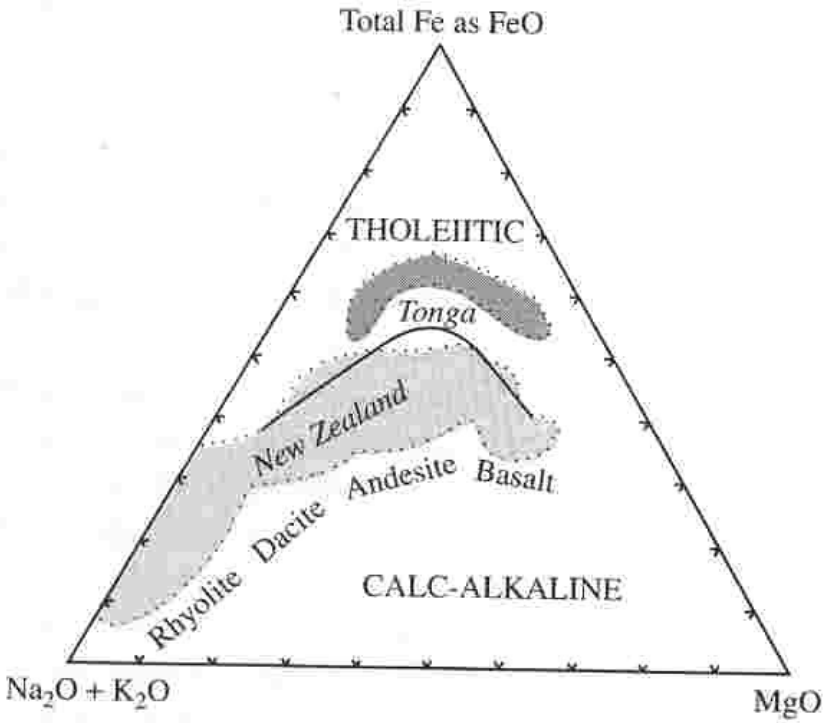

2.17 Subalkaline rocks can be subdivided into **tholeiitic** and **calc-alkaline rock suites. AFM diagram** in terms of alkalies ($Na_2O + K_2O$), total Fe as FeO, and MgO. Solid line separates fields of tholeiitic rocks, exemplified by volcanic rocks from the Tonga island arc in the Pacific Ocean (Figure 2.16), from calc-alkaline rocks, exemplified by most of the volcanic rocks from the North Island of New Zealand. Approximate range of rhyolite, dacite, andesite, and basalt rock types in New Zealand is indicated. Data from Cole (1982).

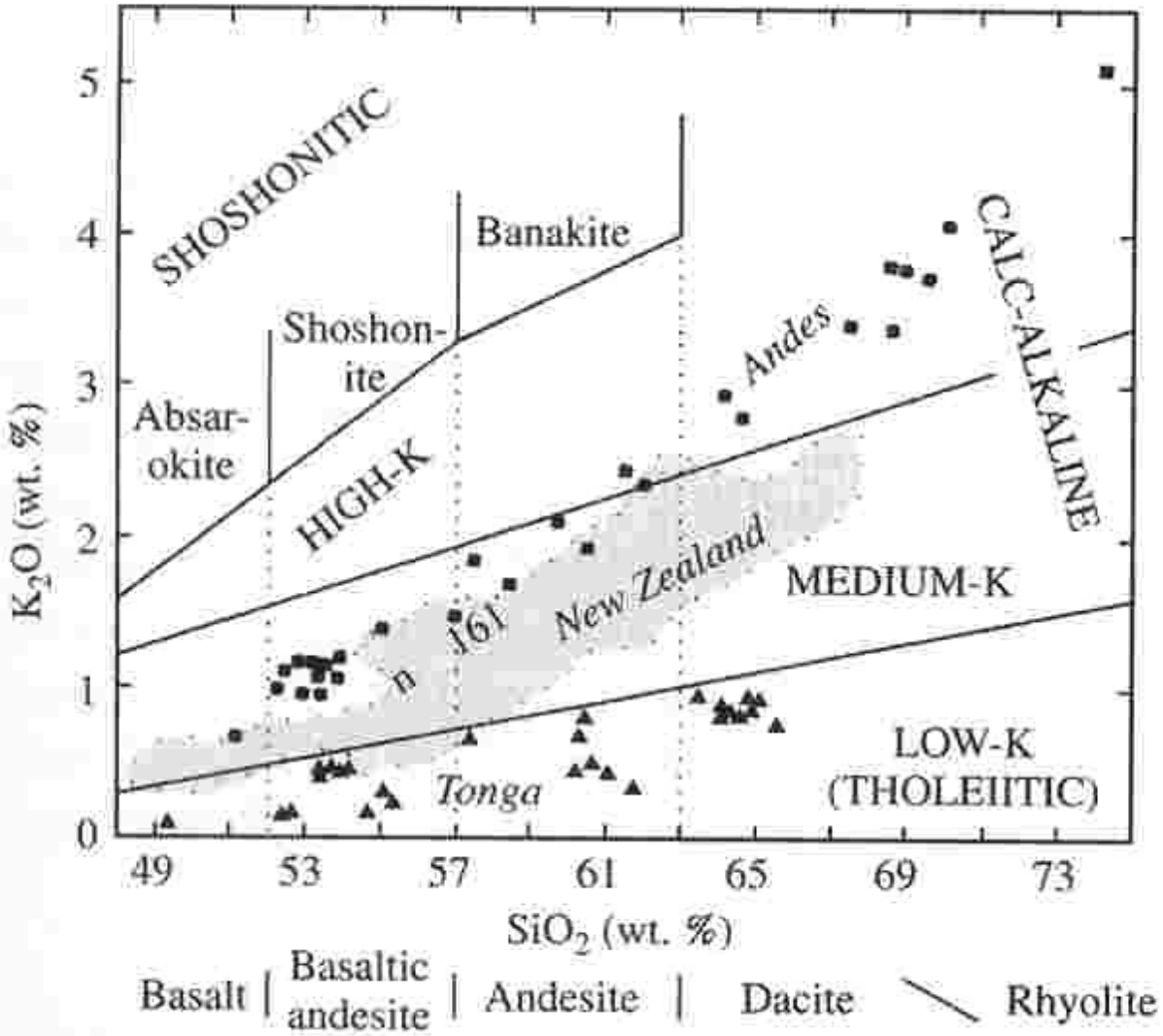
SHOSHONITIC
Banakite
Shoshon-
ite
Absar-
okite
HIGH-K
Andes
CALC-ALKALINE
MEDIUM-K
New Zealand
n
j61
LOW-K
(THOLEIITIC)
Tonga
K_2O (wt. %)
SiO_2 (wt. %)
0
1
2
3
4
5
49
53
57
61
65
69
73
Basalt
Basaltic andesite
Andesite
Dacite
Rhyolite

Table 7–5 Comparisons of a basaltic magma, postulated to be the parental magma for Kilauea Volcano, and a garnet lherzolite that could be a possible source rock for such a basalt. Also given is the calculated composition of the residue left on extraction of the liquid.

	Basalt	Peridotite	Residue
		Major Elements—Wt %	
SiO_2	46.70	44.50	44.44
TiO_2	1.85	1.30	1.29
Al_2O_3	9.17	2.80	2.64
FeO*	11.90	10.30	10.26
MgO	20.00	37.90	37.90
CaO	7.86	3.30	3.18
Na_2O	1.54	0.40	0.37
K_2O	0.40	0.01	0.00
		Trace Elements—ppm	
Ni	855	2300	2337
Cr	1400	3000	3041
Ba	195	5	<0.01
U	0.7	0.02	<0.01
Th	0.3	0.08	<0.01
		Normative and Modal Minerals	
Olivine	5.1	50.6	54.0
Opx	31.9	20.5	18.0
Cpx	32.4	14.3	20.2
Garnet	25.6	14.4	6.5
Phlogopite	3.2	0.2	0.0
Rutile	1.8	0.0	1.3
Density	2.81	3.47	3.46

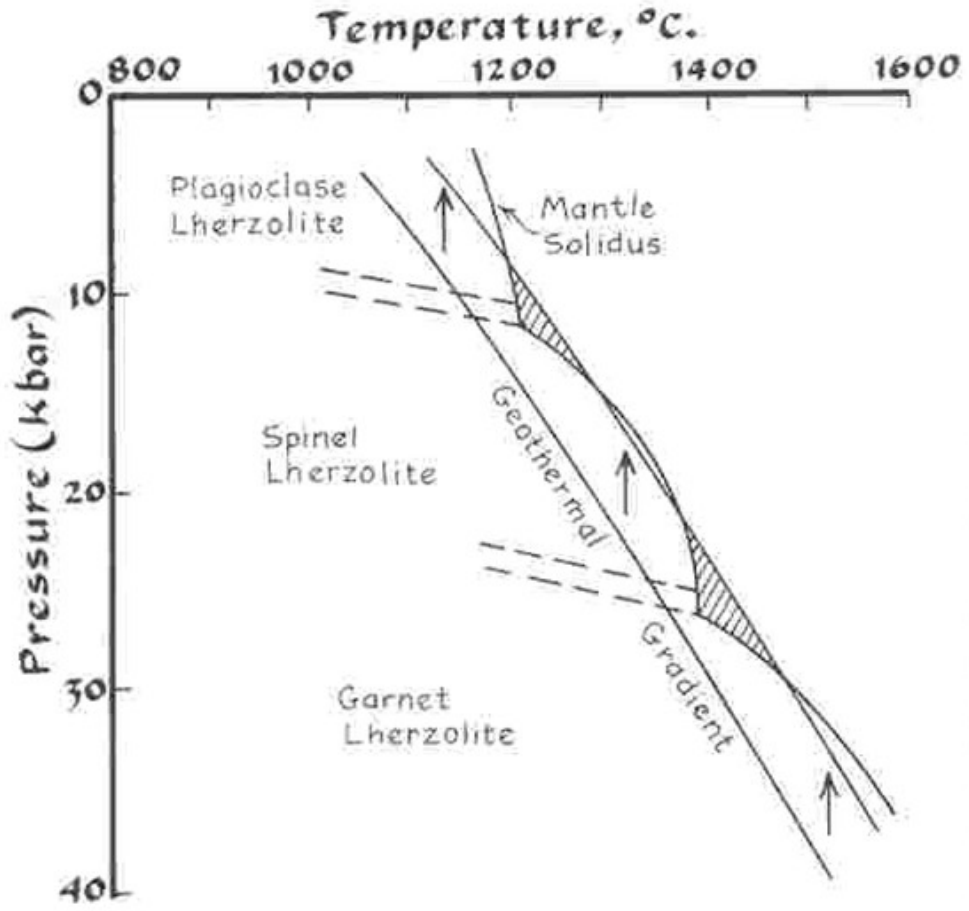

Figure 7-14 Melting at a cusp in the mantle solidus. Note that the change of slope resulting from a transition from one aluminous phase to another causes the solidus to be convex toward the thermal gradient. The levels at which this occurs would be favored places for melting, either by rising temperature, falling pressure, or lowering of the solidus. (Adapted from E. Takahashi and I. Kushiro, 1983, *Amer. Min.* 68:859–879.)

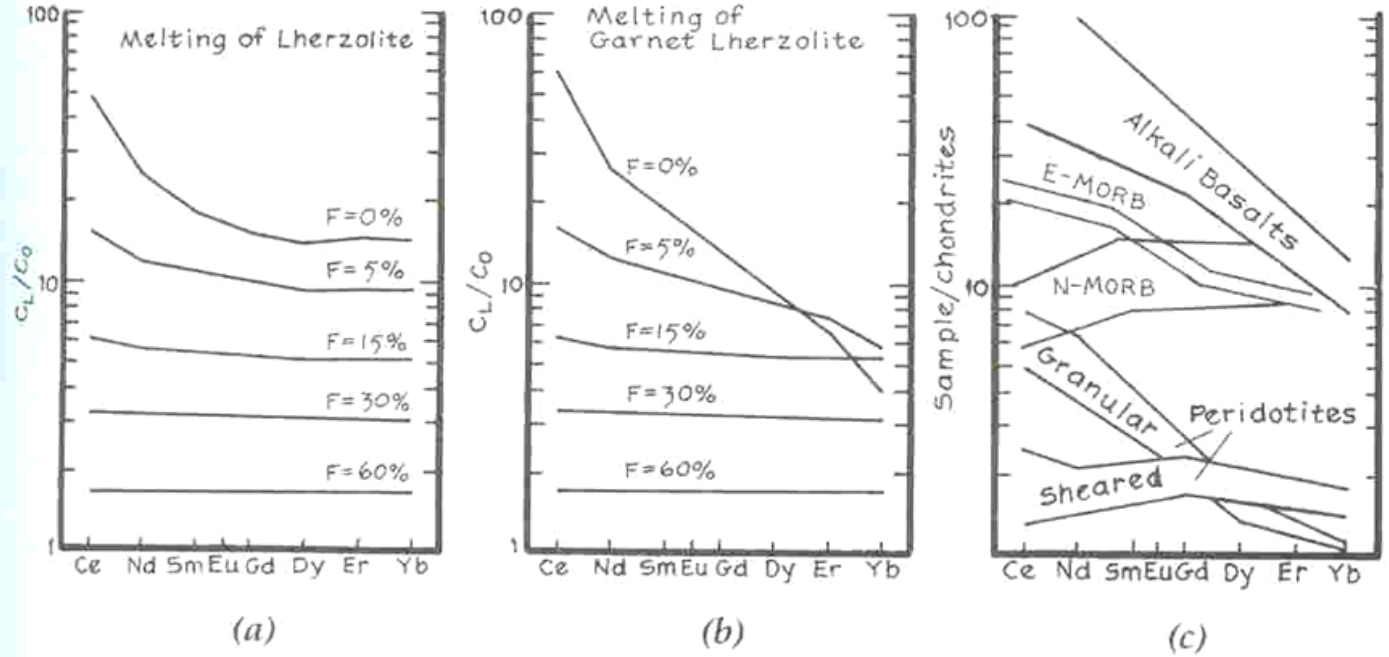

Figure 7–27 Calculated REE distribution patterns for melts derived by batch melting of two lherzolites, one (a) without garnet and another (b) with 5 percent garnet. Note the stronger depletion of heavy REE in small fractions of melt from the garnetiferous lherzolite and the similarity of melts evolved beyond 5 percent melting. Patterns in natural basalts (c) from some intra-plate volcanoes are strongly depleted in heavy REE as one might expect from small amounts of melting of a garnet-bearing source rock, whereas most basalts from mid-ocean ridges (N-MORB) have flatter slopes that could result from melting at shallow levels where garnet is not stable or, alternatively, by advanced degrees of melting. An enriched type of mid-ocean ridge basalt (E-MORB) has a steeper pattern, suggesting a deeper origin where garnet is stable. Abundances of REE in all three diagrams are plotted on logarithmic scales; those of (a) and (b) are normalized to the abundances in the original peridotite, while those in (c) are normalized to the abundances in chondritic meteorites. The differences between abundances in chondritic meteorites and sheared mantle peridotites are not large. (a) and (b) after G. N. Hanson, 1978, *Ann. Rev. Earth Planet. Sci.* 8:371–406.

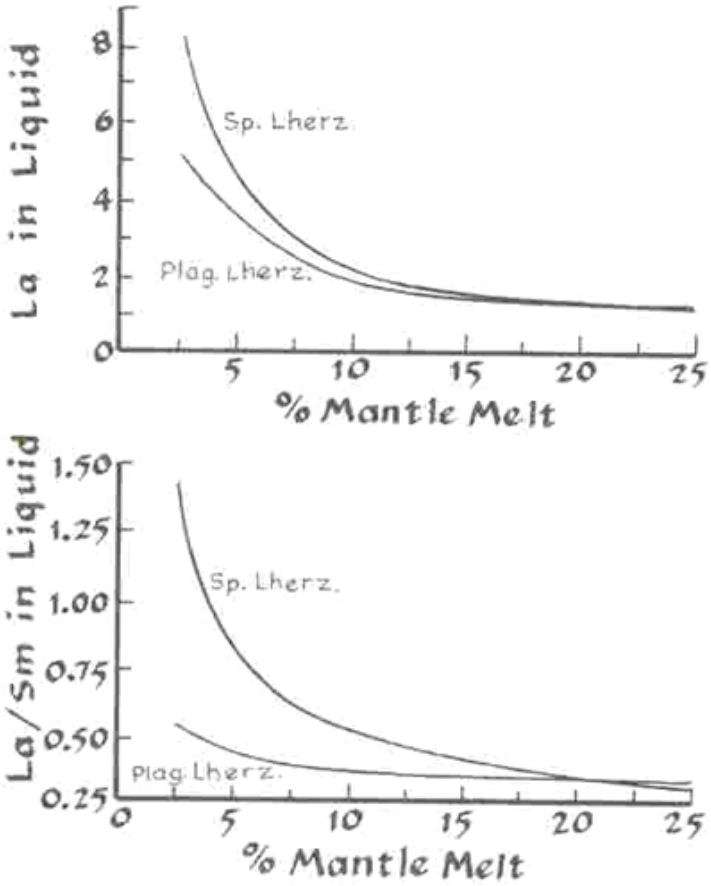

Figure 7–28 (a) Calculated concentrations of La in liquids produced by progressive batch melting of spinel lherzolite and plagioclase lherzolite of the same bulk chemical compositions. (b) La-Sm ratio for the same melts as in (a) La, the lightest of the REE, is not shown in the diagrams of Figure 7–27 but would fall to the left of Ce on the horizontal scale. (After J. F. Allan, R. Batiza, and P. Lonsdale, 1987, *Seamounts, Islands, and Atolls*, Geoph. Mono. 43, Amer. Geoph. Un., 255–282.)

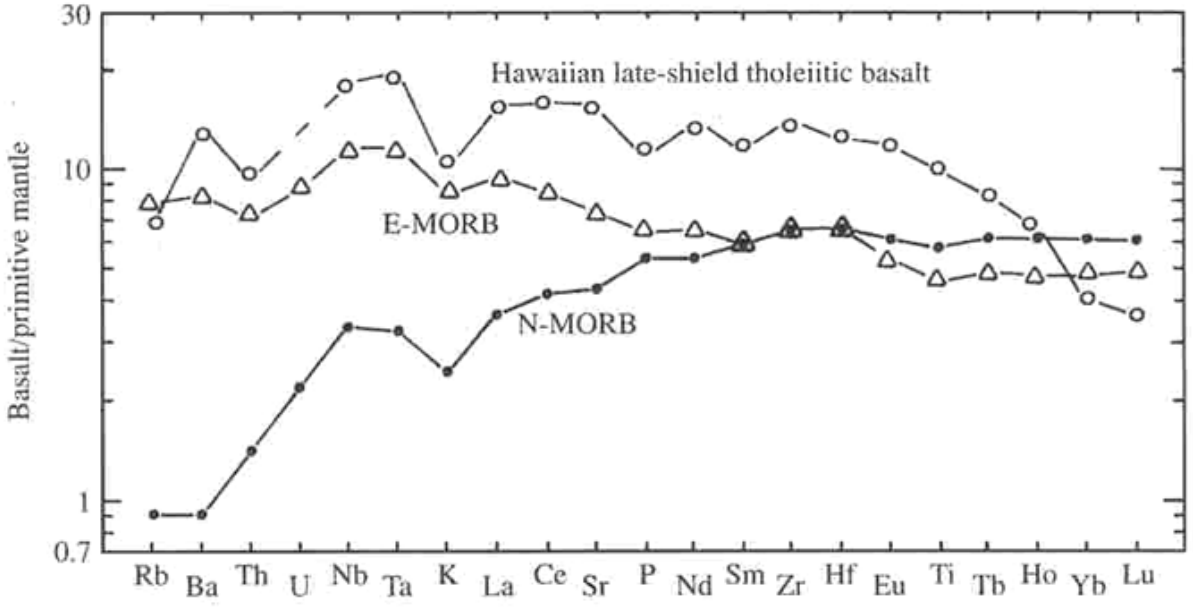

13.2 Primitive-mantle-normalized trace element patterns of oceanic tholeiitic basalts. Decreasing element incompatibility in mafic magmas from left to right. MORB data and normalizing values from Sun and McDonough (1989). Hawaiian tholeiite from Table 13.3.

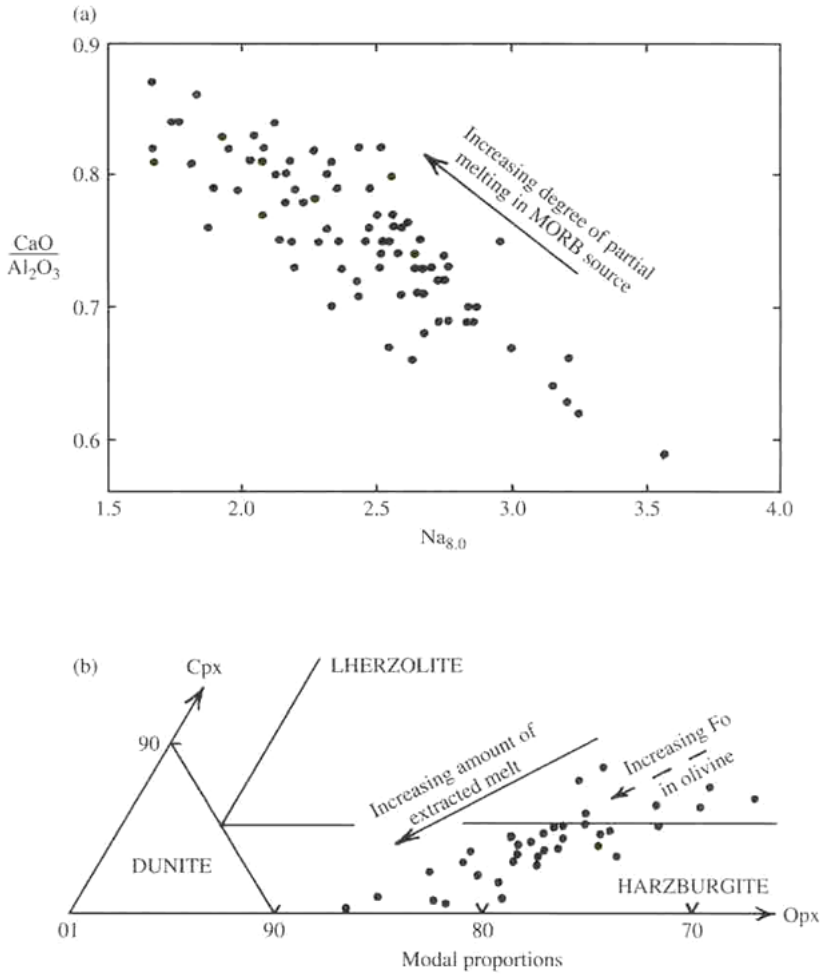

13.3 Compositions of MORB and abyssal peridotite reflect varying degrees of partial melting of the mantle source. (a) Global MORB composition. Variable on the *x* axis is the concentration of Na at 8 wt.% MgO on a Na-MgO variation diagram drawn for 84 sites at spreading ridges around the world (775 samples in all). The CaO/Al_2O_3 ratio is taken from a CaO/Al_2O_3-MgO variation diagram for samples at each site; intrasite variation in the ratio is negligible. (Redrawn from Klein and Langmuir, 1987.) (b) Mineral proportions in abyssal peridotite show that varying amounts of basaltic partial melt have been extracted. Data from Dick et al. (1984). Each point is the average modal proportion of Ol, Cpx, and Opx in 266 samples from 36 dredge-haul sites along rifts in the Atlantic Ocean, Indian Ocean, and Caribbean Sea. The classification diagram is for ultramafic rocks (Figure 2.10b). The most extensively melted peridotite, that is, the most sterile, has least Cpx and Opx and greatest Fo content of olivine (compare Figure 11.9).